micro

Article

Electrical Utilizations of Air Gap Region Formed on Superhydrophobic Silicone Rubber in NaCl Aqueous Solution

Masayuki Okoshi

Department of Electrical and Electronic Engineering, National Defense Academy, 1-10-20 Hashirimizu, Yokosuka 239-8686, Kanagawa, Japan; okoshi@nda.ac.jp

Abstract: A uniform air gap was successfully formed on a superhydrophobic silicone rubber in water or NaCl aqueous solution. The main chain of Si–O bonds of a silicone rubber was photodissociated by a 193 nm ArF excimer laser to lower the molecular weight only in the laser-irradiated microareas; due to the volume expansion, the microswelling structure was periodically fabricated on a silicone rubber, showing the superhydrophobic property. A pair of metal needles were inserted in the air gap formed on the superhydrophobic silicone rubber in a NaCl aqueous solution; an electrical insulation between two metal needles in the air gap was demonstrated. Additionally, a droplet of NaCl aqueous solution was confined in the air gap, after which the pair of metal needles contacted with the droplet through the air gap. As a result, an electrolysis of the droplet of NaCl aqueous solution occurred to produce hydrogen gas on the cathode in the air gap. Moreover, when Al and Cu wires were provided across the air gap and NaCl aqueous solution on the superhydrophobic silicone rubber, approximately 0.8–0.9 V of electric voltage was successfully generated between the two wires in the air gap based on the difference in electrochemical potential as an energy harvesting device in the sea.

Keywords: air gap; superhydrophobic property; silicone rubber; NaCl aqueous solution; electrical insulation; electrolysis; electric voltage; energy harvesting

check for updates

Citation: Okoshi, M. Electrical Utilizations of Air Gap Region Formed on Superhydrophobic Silicone Rubber in NaCl Aqueous Solution. *Micro* **2022**, *2*, 488–494. https://doi.org/10.3390/micro2030030

Academic Editor: Ewa Kowalska

Received: 20 July 2022
Accepted: 8 August 2022
Published: 10 August 2022

1. Introduction

As one of the important properties of material surfaces to be explored, hydrophobic or superhydrophobic properties have been extensively paid attention to for scientific and industrial applications [1,2]. The functional group -CF_3 is the most effective for expressing hydrophobic properties on materials due to its introduction as a chemical modification [3]. However, the contact angle of water on the chemically modified surface should be approximately 120 degrees at the highest [4]. On the other hand, formations of concavo-convex structures on the material, including nanoparticle embedding, nanoneedle formation, and other characteristic structures, are the most practical for obtaining superhydrophobic properties, which shows a contact angle of water of 150 degrees or more [5–7]. This phenomenon follows the Wenzel and Cassie–Baxter equations [8,9]. From the perspective of biomimetics, it can be said that this phenomenon originates from the nature of plants, insects, or reptiles [10]. In recent years, biomimetic superhydrophobic materials have been widely studied by using various unique methods [11–13]. Repelling water from a material and self-cleaning are listed as some potential applications [14,15]. In various methods, laser ablation based on the focused irradiation of intense pulsed lasers is also effective for texturing material surfaces [16,17].

In our previous work, as another approach using lasers, we found that the periodic microswelling structure of silicone rubber can be photochemically formed by a 193 nm ArF excimer laser [18–20]. When the ArF excimer laser irradiated the silicone rubber, the main chain of the Si–O bonds of the silicone rubber could be photodissociated into lower molecules, resulting in the swelling of the laser-irradiated microareas as follows:

$$(SiO(CH_3)_2)_n + h\nu(193\ nm) \rightarrow (SiO(CH_3)_2)_{n-m} + (SiO(CH_3)_2)_m$$

In order to make it periodic, we used silica glass microspheres with a diameter of 2.5 μm, which covered the entire surface of the silicone rubber during the laser irradiation [21]. As a result, the periodic microswelling structure of the silicone rubber showed a superhydrophobic property [19,20]. To develop the potential application in water, we have demonstrated that an air gap layer can be formed on the periodic microswelling structure of the silicone rubber [19,22,23]. In a previous experiment, the periodic microswelling structure was formed on one side of the silicone rubber and the sample was put underwater slowly. Thus, an approximately 0.5-mm-thick air gap layer was automatically formed only on the superhydrophobic surface. In fact, the nonirradiated surface of the silicone rubber did not produce any air gap layers in water. Therefore, the periodic microswelling structure of the silicone rubber successfully repelled water in water. Moreover, the air gap layer could be inflated by an injection of air with a syringe to enable the electrical utilization of the air gap region. In biomimetics, it is known that the skin surface of lizards is highly hydrophobic, and it is possible to promote underwater respiration by using a small amount of air that stays on the hydrophobic skin surface in water [24].

In this paper, the electrical utilizations of the air gap region formed on the periodic microswelling structure of the silicone rubber in water or NaCl aqueous solution are successfully demonstrated. A pair of metal needles are inserted in the air gap in the NaCl aqueous solution and electric voltage is applied to the two needles. An electrical insulation between the two needles in the air gap is shown. Additionally, a droplet of NaCl aqueous solution is confined in the air gap in water and then the pair of metal needles are contacted with the droplet through the air gap. Thus, an electrolysis of the NaCl aqueous solution occurs to produce hydrogen gas on the cathode in the air gap. When Al and Cu wires are provided across the air gap and NaCl aqueous solution on the periodic microswelling structure of the silicone rubber, an electric voltage is successfully generated between the two wires in the air gap based on the difference in electrochemical potential.

2. Preparation of the Superhydrophobic Silicone Rubber

To obtain the superhydrophobic property on the silicone rubber surface, the periodic microswelling structure was fabricated on silicone rubber. Experimentally, silica glass microspheres with a diameter of 2.5 μm (Nippon Shokubai KE-P250) were dispersed in ethanol (99.5% purity) and the dispersed solution was dripped on the surface of a 2-mm-thick silicone rubber of 10 × 10 or 10 × 15 mm^2 [19,22]. Thus, a single layer of the silica glass microspheres was formed on the silicone rubber after air drying, in addition to the removal of excess microspheres by wiping. The sample was placed approximately 80 mm away from the outlet of the ArF excimer laser (Coherent COMPexPro110). The beam path was filled with N_2 gas at a flow rate of 10 L/min to avoid the strong optical absorption of O_2 molecules in the air. The ArF excimer laser irradiated the sample surface without a lens. A single pulse fluence of the ArF excimer laser was approximately 10 mJ/cm^2. The pulse repetition rate and pulse number were 1 Hz and 1800, respectively. The pulse width of the ArF excimer laser was approximately 20 ns. All the laser irradiations were carried out at room temperature. After the laser irradiation, the silica glass microspheres were removed by a 1 wt% HF chemical etching for 90 s.

3. Results and Discussion

3.1. Electrical Insulation in the Air Gap

The superhydrophobic silicone rubber was immersed slowly in water or in 3 wt% NaCl aqueous solution. Then a uniform air gap was formed on the superhydrophobic silicone rubber surface, as shown in Figure 1a. When we observed the sample from a top view, the area of the air gap was slightly smaller than the laser-irradiated area, as well as the shape of the air gap.

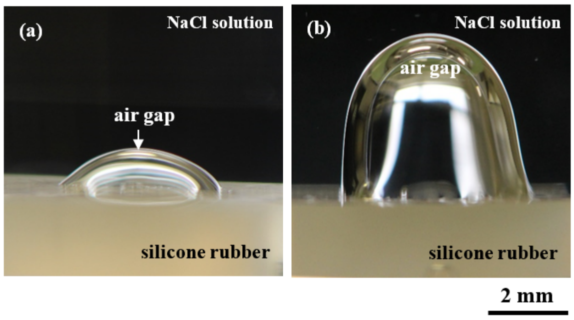

Figure 1. Photographs of the (**a**) air gap and (**b**) inflated air gap formed on the superhydrophobic silicone rubber in 3 wt% NaCl aqueous solution.

From the top view, it was almost circular, even though the laser-irradiated area was a square shape. This might be the result of a small amount of air between the microswelling structures gathering near the center. Moreover, the air gap could be inflated uniformly by an injection of air with a syringe, as shown in Figure 1b. A domed-shape air gap, approximately 4.5 mm wide and 4.0 mm high, was formed. In addition, the inflated air gap was stable in water or in NaCl aqueous solution.

To see if the electrical insulation inside the inflated air gap is maintained, a pair of metal needles were kept approximately 3 mm apart and were inserted into the inflated air gap through the 3 wt% NaCl aqueous solution. An electric voltage was applied to the two needles from 3 to 15 V. We checked whether the electric current is flowing using an mA meter. As shown in Figure 2a and in the insertion photograph on the upper right, the electric current flows between the two needles outside the inflated air gap in the NaCl aqueous solution. On the other hand, as shown in Figure 2b, the electric current did not flow in the inflated air gap even under the electric field of approximately 5 V/mm. For reference, the current flowed in the air gap-free condition under the same electric field. Thus, the electrical insulation was obtained in the inflated air gap formed on the superhydrophobic silicone rubber in a conductive NaCl aqueous solution.

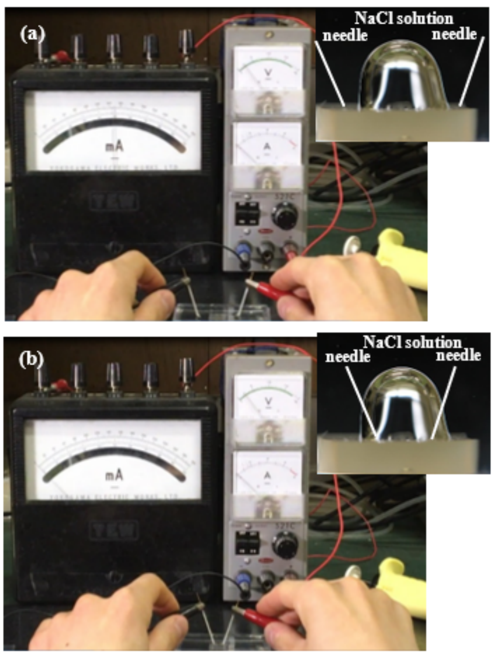

Figure 2. Photographs of the electrical insulation test of the inflated air gap formed on the superhydrophobic silicone rubber in 3 wt% NaCl aqueous solution. A pair of metal needles were placed (**a**) outside and (**b**) inside the inflated air gap. The electric voltage was applied to the two needles from 3 to 15 V.

3.2. Electrolysis of the NaCl Aqueous Solution in the Air Gap

To demonstrate the electrolysis in air gap, at first, the inflated air gap was formed on the superhydrophobic silicone rubber in water. Secondly, a droplet of 3 wt% NaCl aqueous solution was put into the inflated air gap with a syringe, as shown in Figure 3a. After confining the droplet in the inflated air gap, the shape of the inflated air gap was slightly changed by inserting and removing the syringe, compared with the case in Figure 1b. Then, a pair of metal needles were inserted in the water and gradually reached the droplet (Figure 3b). An electric voltage of 15 V was applied to the two needles. As a result, as shown in Figure 3c, hydrogen gas could be generated on the cathode. In addition, a very small amount of chlorine gas might also be generated on the anode. Therefore, the electrolysis of the droplet of NaCl aqueous solution successfully occurred in the inflated air gap. In practical use, a droplet of water confined in the inflated air gap may be more useful for the present millimeter-sized electrolysis.

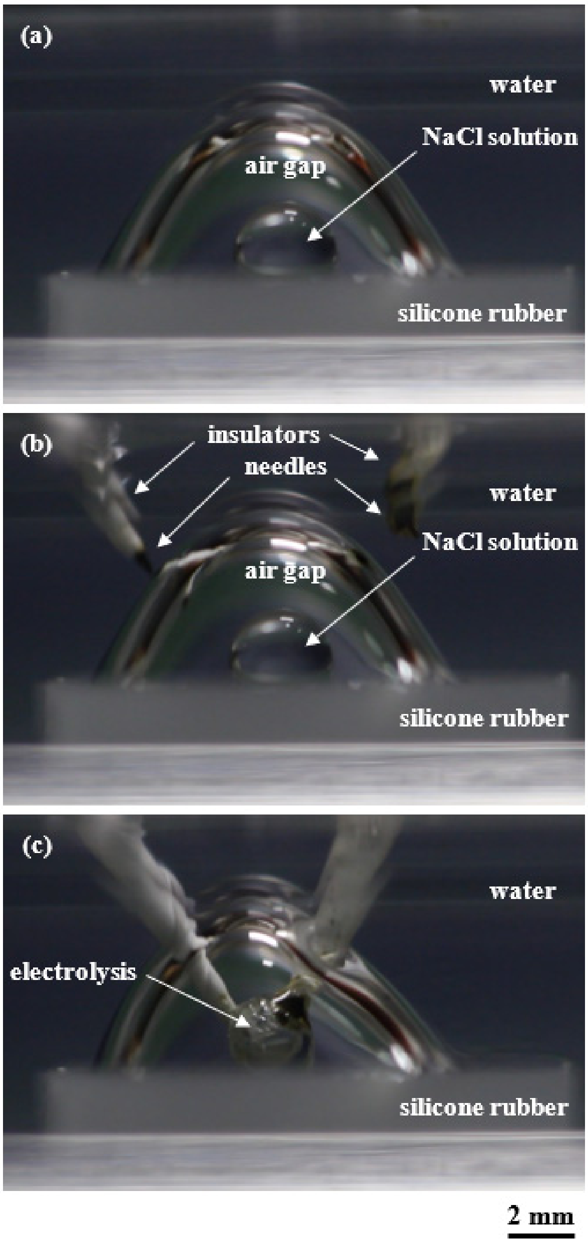

Figure 3. Photographs of the (**a**) droplet of NaCl aqueous solution confined in the inflated air gap, (**b**) reaching a pair of metal needles to the droplet through water, and (**c**) applying the electric voltage of 15 V to the droplet to initiate the electrolysis.

3.3. Generation of Electric Voltage in the Air Gap

Considering the inflated air gap is surrounded by a conductive NaCl aqueous solution, we decided to use two different metal wires, which are provided across the inflated air gap and the NaCl aqueous solution on the superhydrophobic silicone rubber. In other words, the generation of electric voltage between the two electrodes in the inflated air gap was harvested from the NaCl aqueous solution based on the difference in electrochemical potential. Figure 4a,b show the cross-sectional and top-view illustrations of the generation of electric voltage in the inflated air gap in the NaCl aqueous solution, respectively. Figure 4c also shows the top-view photograph of the setup before immersing in the NaCl aqueous solution. In the present experiment, an Al wire of 1.0 mm in diameter and a Cu wire of 0.7 mm in diameter were used. After immersing the sample in 3 wt% NaCl aqueous solution, approximately 0.8–0.9 V of electric voltage was successfully generated in the inflated air gap. The standard electrode potential of Al is as follows:

$$Al^{3+} + 3e^- \rightarrow Al\ (E^0 = -1.676\ V)$$

On the other hand, on the Cu electrode, it is considered that the following reaction is occurring:

$$H_2O + e^- \rightarrow \frac{1}{2}H_2 + OH^-(E^0 = -0.828\ V)$$

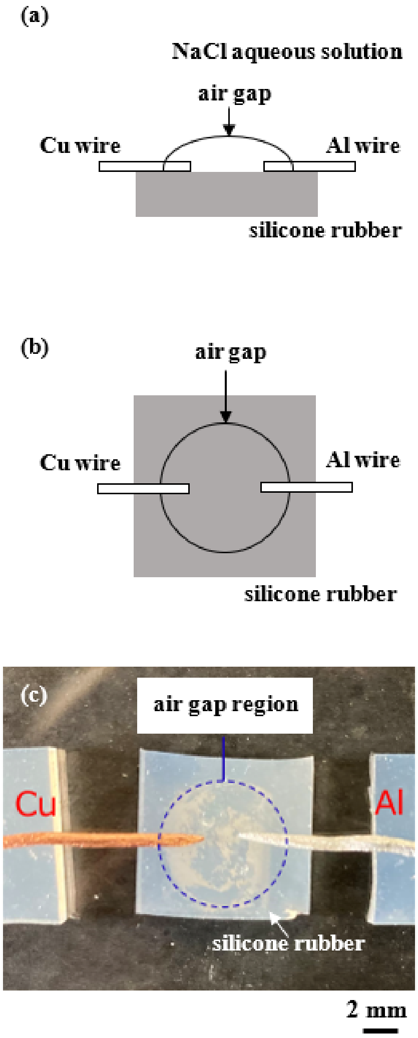

Figure 4. (**a**) Cross-sectional and (**b**) top-view illustrations of the generation of electric voltage in the inflated air gap in the NaCl aqueous solution, in addition to the (**c**) top-view photograph of the setup before immersing in the NaCl aqueous solution.

As a result, the ideal generated electric voltage is estimated to be 0.848 V. Thus, the obtained voltage of 0.8–0.9 V was almost agreed with the estimated electric voltage of 0.848 V. Therefore, the generation of electric voltage was successfully demonstrated in the inflated air gap in the NaCl aqueous solution. This result is considered for use as an energy harvesting application for an Internet of Things (IoT) device in the sea.

4. Conclusions

The electrical utilizations of the air gap region formed on the superhydrophobic silicone rubber in water or in NaCl aqueous solution were demonstrated. The superhydrophobic property was obtained by the 193 nm ArF excimer laser-induced photodissociation of the silicone rubber; the periodic microswelling structure was photochemically fabricated on the silicone rubber to repel water in water. A pair of metal needles were inserted in the air gap formed on the superhydrophobic silicone rubber in 3 wt% NaCl aqueous solution; the electrical insulation between the two metal needles under the approximately 5 V/mm electric field in the air gap was shown. A droplet of the NaCl aqueous solution was confined in the air gap and then the pair of metal needles were contacted with the droplet through the air gap. As a result, the electrolysis of the droplet of the NaCl aqueous solution occurred to produce hydrogen gas on the cathode in the air gap. Moreover, when the Al and Cu wires were provided across the air gap and NaCl aqueous solution on the superhydrophobic silicone rubber, approximately 0.8–0.9 V of electric voltage was successfully generated between the two wires in the air gap based on the difference in electrochemical potential. The results enable the development of an energy harvesting device in water or in NaCl aqueous solution and are applicable to a potential IoT device that works in the sea.

Funding: This work was supported by JSPS KAKENHI Grant Number JP21K04732.

Data Availability Statement: The data that support the findings of this study are available from the corresponding author upon reasonable request.

Acknowledgments: The author acknowledges Wisnu Setyo Pambudi, Masateru Miyoshi, Kohei Yamashita, and Yuto Yamamoto, National Defense Academy, for helpful assistance and valuable discussion.

Conflicts of Interest: The author declares no conflict of interest.

References

1. Bhutani, G.; Muralidhar, K.; Khandekar, S. *Drop Dynamics and Dropwise Condensation on Textured Surfaces*; Springer: Cham, Switzerland, 2020.
2. Chu, F. *Condensed and Melting Droplet Behavior on Superhydrophobic Surfaces*; Springer: Singapore, 2021.
3. Katasho, Y.; Liang, Y.; Murata, S.; Fukunaka, Y.; Matsuoka, T.; Takahashi, S. Mechanisms for enhanced hydrophobicity by atomic-scale roughness. *Sci. Rep.* **2015**, *5*, 13790. [CrossRef] [PubMed]
4. Nishino, T.; Meguro, M.; Nakamae, K.; Matsushita, M.; Ueda, Y. The lowest surface free energy based on $-CF_3$ alignment. *Langmuir* **1999**, *15*, 4321–4323. [CrossRef]
5. Karapanagiotis, I.; Manoudis, P. Superhydrophobic and Water-Repellent Polymer-Nanoparticle Composite Films. In *Industrial Applications for Intelligent Polymers and Coatings*; Hosseini, M., Makhlouf, A.S.H., Eds.; Springer: Cham, Switzerland, 2016; pp. 205–221.
6. Narhe, R.D.; Beysens, D.A. Water condensation on a super-hydrophobic spike surface. *EPL* **2006**, *75*, 98–104. [CrossRef]
7. Parvate, S.; Dixit, P.; Chattopadhyay, S. Superhydrophobic surfaces: Insights from theory and experiment. *J. Phys. Chem. B* **2020**, *124*, 1323–1360. [CrossRef] [PubMed]
8. Wenzel, R.N. Resistance of solid surfaces to wetting by water. *Ind. Eng. Chem.* **1936**, *28*, 988–994. [CrossRef]
9. Cassie, A.B.D.; Baxter, S. Wettability of porous surfaces. *Trans. Faraday Soc.* **1944**, *40*, 546–551. [CrossRef]
10. Darmanin, T.; Guittard, F. Superhydrophobic and superoleophobic properties in nature. *Mater. Today* **2015**, *18*, 273–285. [CrossRef]
11. Li, S.; Tian, Z.; Liu, X.; Han, Z.; Ren, L. Biomimetic superhydrophobic and antibacterial stainless-steel mesh via double-potentiostatic electrodeposition and modification. *Surf. Coat. Technol.* **2020**, *403*, 126355. [CrossRef]
12. Du, X.; Xin, B.; Xu, J.; Wang, C. Biomimetic superhydrophobic membrane with multi-scale porous microstructure for waterproof and breathable application. *Colloids Surf. A Physicochem. Eng. Asp.* **2021**, *612*, 125924. [CrossRef]
13. Wu, Y.; Dong, L.; Shu, X.; Yang, Y.; She, W.; Ran, Q. A review on recent advances in the fabrication and evaluation of superhydrophobic concrete. *Compos. B. Eng.* **2022**, *237*, 109867. [CrossRef]

14. Hong, X.; Hu, H.; Yan Gao, Y. Thermodynamic analysis and prediction on the wetting properties of pore array superhydrophobic laser-texturing surfaces. *J. Appl. Phys.* **2021**, *129*, 215302. [CrossRef]
15. Latthe, S.S.; Sutar, R.S.; Kodag, V.S.; Bhosale, A.K.; Kumar, A.M.; Sadasivuni, K.K.; Xing, R.; Liu, S. Self-cleaning superhydrophobic coatings: Potential industrial applications. *Prog. Org. Coat.* **2019**, *128*, 52–58. [CrossRef]
16. Vercillo, V.; Cardoso, J.T.; Huerta-Murillo, D.; Tonnicchia, S.; Laroche, A.; Guillén, J.A.M.; Ocaña, J.L.; Lasagni, A.F.; Bonaccurso, E. Durability of superhydrophobic laser-treated metal surfaces under icing conditions. *Mater. Lett. X* **2019**, *3*, 100021. [CrossRef]
17. Cao, M.; Guo, D.; Yu, C.; Li, K.; Liu, M.; Jiang, L. Water-repellent properties of superhydrophobic and lubricant-infused "slippery" surfaces: A brief study on the functions and applications. *ACS Appl. Mater. Interfaces* **2016**, *8*, 3615–3623. [CrossRef] [PubMed]
18. Takao, H.; Okoshi, M.; Inoue, N. Swelling and modification of silicone surface by F_2 laser irradiation. *Appl. Phys. A* **2004**, *79*, 1571–1574. [CrossRef]
19. Okoshi, M.; Pambudi, W.S. Fabrication of superhydrophobic silicone rubber by ArF-excimer-laser-induced microstructuring for repelling water in water. *Appl. Phys. Express* **2016**, *9*, 112701. [CrossRef]
20. Nojiri, H.; Pambudi, W.S.; Okoshi, M. Formation of periodic micro-swelling structures on silicone rubber surface by ArF excimer laser to realize superhydrophobic property. *Jpn. J. Appl. Phys.* **2017**, *56*, 072002. [CrossRef]
21. Okoshi, M.; Awaihara, Y.; Yamashita, T.; Inoue, N. F_2-laser-induced micro/nanostructuring and surface modification of iron thin film to realize hydrophobic and corrosion resistant. *Jpn. J. Appl. Phys.* **2014**, *53*, 112701. [CrossRef]
22. Okoshi, M. Fabrication of superhydrophobic silicone rubber operating in water. *Appl. Phys. Express* **2018**, *11*, 101801. [CrossRef]
23. Okoshi, M. Formation of textured Al thin film on silicone rubber to obtain superhydrophobic property. *SN Appl. Sci.* **2018**, *1*, 133. [CrossRef]
24. Boccia, C.K.; Swierk, L.; Varela, F.P.A.; Boccia, J.; Borges, I.L.; Estupiñán, C.A.; Martin, A.M.; Grimaldo, R.E.M.; Ovalle, S.; Senthivasan, S.; et al. Repeated evolution of underwater rebreathing in diving Anolis lizards. *Curr. Biol.* **2021**, *31*, 2947–2954. [CrossRef] [PubMed]